Novel Biocement/Honey Composites for Bone Regenerative Medicine

Lubomir Medvecky , Maria Giretova , Radoslava Stulajterova * , Tibor Sopcak , Pavlina Jevinova , Lenka Luptakova

Posted Date: 28 July 2023

doi: 10.20944/preprints202307.1894.v1

Keywords: biocement; honey; antimicrobial properties; antioxidant properties; osteogenic potential

Article

Novel Biocement/Honey Composites for Bone Regenerative Medicine

Lubomir Medvecky [1], Maria Giretova [1], Radoslava Stulajterova [1,*], Tibor Sopcak [1], Pavlina Jevinova [2] and Lenka Luptakova [3]

[1] Division of Functional and Hybrid Systems, Institute of Materials Research of SAS, Watsonova 47, 040 01 Kosice, Slovakia; lmedvecky@saske.sk, mgiretova@saske.sk, rstulajterova@saske.sk, tsopcak@saske.sk

[2] Department of Food Hygiene, Technology and Safety, University of Veterinary Medicine and Pharmacy, Komenskeho 73, 041 81, Kosice, Slovakia; pavlina.jevinova@uvlf.sk

[3] Department of Biology and Physiology, University of Veterinary Medicine and Pharmacy in Kosice, Komenskeho 73, 041 81 Kosice, Slovakia; lenka.luptakova@uvlf.sk

* Correspondence: rstulajterova@saske.sk (R.S.)

Abstract: New biocements based on a powdered mixture of calcium phosphate/monetite (TTCPM) modified with the honey addition were prepared by mixing the powder and honey liquid components at a non-cytotoxic concentration of honey (up to 10% (w/v)). The setting process of the cements was not affected by the addition of honey, and the setting time of ~4 min corresponded to the fast setting calcium phosphate cements (CPC's). The cement powder mixture was completely transformed into calcium-deficient nanohydroxyapatite after 24 hours of hardening in simulated body fluid, and columnar growth of long needle-like nanohydroxyapatite particles around the original calcium phosphate particles was observed in honey cements. The compressive strength of honey cements was reduced with the content of honey in the cement. The comparable antibacterial activity of cements with honey solutions was found on *Escherichia coli*, but very low antibacterial activity was found for *Staphylococus aureus* for all cements. The enhanced antioxidant inhibitory activity of composite extracts was verified. In vitro cytotoxicity testing verified the non-cytotoxic nature of honey cement extracts, and the addition of honey promoted alkaline phosphatase activity, calcium deposit production, and upregulation of osteogenic genes (osteopontin, osteocalcin, and osteonectin) by mesenchymal stem cells, demonstrating a positive synergistic effect of honey and CPC on the bioactivity of cements that could be promising therapeutic candidates for the repair of bone defects.

Keywords: biocement; honey; antimicrobial properties; antioxidant properties; osteogenic potential

1. Introduction

The large critical bone defects (>2 cm in diameter in humans) cannot be repaired spontaneously by reparative mechanisms and need to help from outside in the form of grafts or scaffolds, with appropriate biological and mechanical properties, preferably supplemented with cells and growth factors [1,2]. Nearly 2 million of bone grafts (autografts, allografts or xenografts) are performed worldwide per year. Autograft are still considered as gold standard but caused bleeding, haematoma and pain due to the invasiveness of the surgical technique, but on the other hand, allografts and xenografts may cause the risk of disease transmission or immunological reaction. However, no scaffold is considered the best candidate for healing large bone defects, as bone tissue healing is affected by the patient's age, lifestyle, and overall health [3]. Calcium phosphate cements (CPC) belong to an important class of biomaterials, which are characterized by excellent biocompatibility and osteoconductivity, non-cytotoxicity and bioresorption, which predetermines them to possible use in the human body for bone repair and replacement [4]. CPC generally consist of a powder and a liquid component that are mixed together to form a paste which can optimally fit the bone defects regardless of their shape [5]. The one of kind CPC is based on mixture basic tetracalcium phosphate (TTCP) and acidic brushite or monetite (DCPA) which are transformed during setting to the nanocrystalline calcium-deficient hydroxyapatite (CDHA). CDHA is chemically and structurally

similar to the mineral component of mammalian bone. It has been shown that fast-setting tetracalcium phosphate/monetite (TTCPM) biocements, especially with modified composition, can promote the osteogenic differentiation of mesenchymal stem cells into osteoblasts [6,7]. On the other hand, adding some heavy metal ions or increasing the pH during the setting process improved the antimicrobial activity of CPC [8–10].

The honey is one of the most complex natural foods, and contains more than 200 substances and composition strongly depends on the botanical and geographical origin [11,12]. Honey has been found to stimulate the healing of wounds and burns and is also effective in treatment of infected wounds [13]. The main constituents of honey are sugars (~ 80%), water (20%) and other ingredients, such as proteins (enzymes), organic acids, vitamins, minerals, pigments, phenolic compounds etc. The phenolic compounds are responsible for diverse color, flavor, antioxidant and antimicrobial properties [14]. The acidity of honey (pH 3.2–4.5) increases its antibacterial properties, since the appropriate pH for the growth of most bacterial strains is 6.5–7.5. It was found that the inhibition of microbial growth caused by honey was attribute by H_2O_2 as well as various non-peroxide substances (phenolic compounds, organic acids, flavonoids) and important supporting factors are also low water content (high osmolarity), high concentration of sugars, the presence of bee defensin-1, and methylglyoxal [15–17]. In addition, the positive effects of honey on bone metabolism, osteoporosis and bone fracture healing have been demonstrated [18–20], but despite these facts, few papers focused on the analysis of the effect of honey addition on the properties of bioactive cements have been published so far.

The aim of this work was to evaluate the properties of a new composite cement based on TTCP/monetitic cement mixture with the addition of honey, where calcium phosphates support the bioactivity of cells through calcium and phosphate ions and, on the other hand, honey can influence the behavior of cells in terms of osteogenic activity, as well as antibacterial and antioxidant properties of cement because of the presence of specific components of honey, such as polyphenols or flavonoids. In the paper, the effect of honey addition (two kinds of honey) on setting process, microstructure, mechanical and antibacterial properties, in vitro cytotoxicity of cements and osteogenic activity of cells cultured in cement extracts was studied.

2. Materials and Methods

2.1. Preparation of cement powder mixture

The tetracalcium phosphate/monetite cement powder mixture (Ca/P mole ratio = 1.67) was synthesized in situ by mixing of tetracalcium phosphate (TTCP) with a diluted ethanolic solution (80% ethanol) of the orthophosphoric acid (86% analytical grade, Merck, Darmstadt, Germany) in the planetary ball mill (Retsch, 600 rpm, agate balls and vessel for 30 min at room temperature). The final powder mixture was composed of TTCP and monetite (DCPA) in equimolar ratio. Tetracalcium phosphate was synthesized by the solid state reaction between calcium carbonate ($CaCO_3$, analytical grade, Sigma Aldrich, Saint Louis, MO, USA) and calcium hydrogen phosphate anhydrous (monetite, DCPA) ($CaHPO_4$ (Ph.Eur., Fluka) at 1450 °C for 5 h. The synthesized TTCP before further treatment was milled in a planetary ball mill (Retsch PM100, 350 rpm) for 1 hour.

2.2. Formation of cement pastes and characterization of honeys

2.2.1. Preparation of cement pastes

The liquid component for the preparation of cement pastes was a 2% solution of NaH_2PO_4 (analytical grade, Sigma-Aldrich, Steinheim, Germany) and honeys were also dissolved in this solution. The two kinds of medical honey were selected and used in study: manuka based honey (Activion®. medical grade, Advancis medical, UK) and chestnut honey (Vivamel®, Tosama, medical grade, Slovenija). The content of honey in the liquid component was 5 and 10 % (w/v); the powder to liquid (P/L) ratio was 2. Cements prepared with 5 and 10% (w/v) honey in the liquid component were

 doi:10.20944/preprints202307.1894.v1

designated as M5, V5 or M10, V10, where M and V represent manuka and chestnut honey, respectively.

2.2.2. Analysis of proteins in honeys

The total content of proteins in honeys was determined using Coomasie blue method [21] and bovine serum albumin as standard; the molecular mass protein profile was analysed by the SDS PAGE gel electrophoresis on polyacrylamide gels (NuPAGE, 4-12 % Bis-Tris gel, 1 mm, Invitrogen, USA) with NuPAGE MOPS running buffer in X´CellSurelock MiniCell (200V, 100 mA for 45 min) at native conditions using NuPAGE LDS sample buffer according to manufacturer conditions. The silver staining (SilverXpress, Invitrogen, USA) was used for detection of proteins in gel and the molecular mass of proteins was standardized by the Novex sharp unstained protein standard kit (Invitrogen, USA). The proteins in dissolved honeys (200 mg/1.5 mL of final solution) were before analysis precipitated with saturated $(NH_4)_2SO_4$ solution and kept at 4 °C for 12 hours, centrifuged at 10000 rpm (HETTICH, Mikro220R, Germany) and recovered in distiled water. The image analysis was used for profile analysis of proteins in lanes (ImageJ 8 softvare).

2.2.3. Determination of total phenols, flavonoids and sugars in honeys and cement extracts during release to SBF

The total amount of polyphenols in honeys and cement extracts during soaking in SBF was determined by Folin-Ciocalteu reagent (FC) [22,23]. Briefly, 100 µL FC was added to 100 µL 10 % (w/v) honey aqueous solution and following 200 µL 5% (w/v) Na_2CO_3 solution was admixed to mixture. After 30 min, the absorbance of reaction mixture was measured at 750 nm using UV VIS spectrophotometer (SHIMADZU, UV VIS 1800, Japan). The gallic acid was selected as a standard for calibration and results were expressed in µg of GAE/g of honey.

The content of flavonoids in honeys was analysed method based on the formation of complexes with $AlCl_3$ [24,25]. 1 mL of 12% (w/v) of honey was mixed with 300 µL of $NaNO_2$ solution (5 % w/v) and after 5 min, the 10 % (w/v) $AlCl_3$ solution was added to reaction mixture . In the last step, 2 mL 10% (w/v) Na_2CO_3 solution was added. The reactants in the solution were mixed together and the content of flavonoids was calculated from calibration curve using quercetin (QUE) as a standard. The results were expressed as µg of QUE/g of honey.

The profil of phenolic compounds in honeys and cement extracts after soaking in 0.9 % NaCl solution was determined by HPLC chromatography. HPLC analysis was performed by using a liquid chromatograph (Watrex), equipped with a multichannel UV VIS detector (SYKAM, S3240, Germany), binary pumps (DeltaChrom), an online vacuum degasser (Watrex), Nucleosil 100-5C18, 4.6×250 mm column (Supelco, UK), at a flow-rate of 1 mL min^{-1} and results were evaluated by the Clarity Datastation Software. Solvent gradient was performed by varying the proportion of solvent A (0.5% formic acid in water (v/v)) to solvent B (methanol) as follows: initial 95% A; 0-20 min, 95 -30% A; 20-25 min, 30–10% A; 25 -30 min, 10-5% A. The total running time and post-running time were 35 and 10 min, respectively. The injected volume of samples and standards was 20 µL. The four wavelenghts at 250, 270,320 and 370 nm were selected for detection of polyphenols.

The honey cement extracts were prepared by soaking of cement pastes (composed of 1 g of powder cement mixture and 500 µL of liquid component with 10 % (w/v) content of honey (V10, M10)) in 10 mL of pure 0.9 % NaCl solution to eliminate any artifacts in the HPLC chromatograms from possible impurities in used organic additives. The solution after the selected soaking time (3, 24, 48, 120 and 168 hours) was filtered through a PVDF membrane filter (Millipore, pore size 0.22 µm) and polyphenols were extracted from the soaking solution by solid phase extraction (SPE cartridge, Bond Elut C18 , 100 mg, Agilent Technologies, USA) according to the manufacturer's instructions. The final ~1 mL methanol solution containing the polyphenols was lyophilized and the polyphenols redissolved in 200 µL methanol. For a more accurate analysis, the recovery of individual selected polyphenolic compounds after SPE extraction was determined using 1 and 10 µg polyphenol/10 ml solution under the same conditions used for the extraction of compounds from soaking solutions, and the results from HPLC analysis were corrected by the corresponding degree of recovery. The

Preprints (www.preprints.org) | NOT PEER-REVIEWED | Posted: 28 July 2023 doi:10.20944/preprints202307.1894.v1

released amount of selected polyphenolic acids and flavonoids from cements during soaking in 0.9 % NaCl solution was expressed relative to total content of polyphenols in cement pastes.

In addition, the filtrates containing the solution of separated sugars after the extraction of polyphenols by SPE were used for the analysis of sugars in honeys and the sugar content in cement extracts during soaking. HPLC chromatography with SupelcoSIL LC-NH2, column 4.6 x 250 mm, size 5 μm and isocratic analysis conditions with mobile phase water:acetonitrile (25:75), RI detector (RI200, Schambeck GmbH, Germany) and 1 ml/min flow rate was used to determine the sugar content in the samples. The released amount of sugars from cements during soaking in 0.9 % NaCl solution was expressed relative to total content of individual sugars in cement pastes.

2.2.4. Free radical scavenging activity and total antioxidant content

The free radical scavenging activity (FRSA) of honeys was characterized by $DPPH^{\bullet}$ (1,1-diphenyl-2-picrylhydrazyl) and $ABTS^{\bullet+}$ (2,2′-azinobis-3-ethylbenzothiazoline-6-sulphuric acid) radical scavenging assays whereas the FRSA of cement extracts after soaking in SBF at selected time periods (1,2,5 and 7 days) was determined using $ABTS^{\bullet+}$ assay only. This method was applied because the reactive $ABTS^{\bullet+}$ radical as well as the final products are soluble in aqueous solution (SBF) in which the release of active substances (e.g., polyphenols) was measured and such experimental conditions were more similar to the physiological environment. On the other hand, the $DPPH^{\bullet}$ assay, which is soluble in organic solvents, is appropriate for the analysis of lipophilic antioxidants (insoluble in water solutions) [26,27]. However, it is unlikely to assume a high activity of water-insoluble substances without some degree of conversion by metabolic processes.

Briefly, 500 μL of 2.5 % (w/v) honey methanolic solution was mixed with 1 mL of 0.06 mM DPPH methanolic solution and the absorbance of solution was measured at 517 nm by UV VIS spectrophotometer (UV VIS 1800, Shimadzu, Japan) after 15 min reaction. In the case of $ABTS^{\bullet+}$ method, 100μL of 2.5 % (w/v) of honey solution or cement extract was reacted with 1 mL of $ABTS^{\bullet+}$ reagent and absorbance at 734 nm was measured after 15 min of reaction. The $ABTS^{\bullet+}$ reagent was prepared by dilution of origin $ABTS^{\bullet+}$ stock solution with phosphate buffer saline (PBS). The reactive $ABTS^{\bullet+}$ radical was synthesized by reacting a 7 mM ABTS solution (5mL) with 140 mM $K_2S_2O_8$ (88 μL) in a molar ratio of 1:0.5 at room temperature for 12 hours [27].

The total antioxidant content (TAC) in honeys and cement extracts was determined by ABTS method where the ascorbic acid (0–10 μg/ml) was used as a standard for calibration and results were expressed in ascorbic acid antioxidant content equivalents (AAE) (mg of ascorbic acid per gram of honey).

The cement extracts for FRSA and TAC analysis were obtained from cement pastes composed of 2.5 g of cement powder mixture and 1.25 mL of 10 % (w/v) honey dissolved in 2 % (w/v) NaH_2PO_4 solution during soaking in 10 mL SBF for 1, 2, 5 and 7 days.

2.2.5. Characterization of microstructure, setting time and mechanical properties

The compressive strength (CS) of cements was measured on a universal testing machine (5 kN load cell, LR5K Plus, Lloyd Instruments Ltd., West Sussex, UK) at crosshead speed of 1 mm/min (mean+standard deviation, n=4). The samples for measurement were prepared from the cement pastes by packing in stainless cylindrical form (6 mm D x 12 mm H), hardening in 100% humidity at 37 °C for 10 min and soaking in simulate body fluid (SBF) at 37 °C for 1 week. The phase composition of samples was characterized by X-ray diffraction analysis (Philips X PertPro, Malvern Panalytical B.V., Eindhoven, the Netherlands, using Cu Kα radiation, 50 mA, 2Θ range 20–40°) and FTIR spectroscopy (IRAffinity1, Shimadzu, Kyoto, Japan, 400 mg KBr + 1 mg sample).

The final cement microstructures of fractured surfaces were observed by the field emission scanning electron microscopy (JEOL FE SEM JSM-7000F, Tokyo, Japan) after coating with carbon. The morphology of calcium phosphosphate particles in cements was analysed by transmission electron microscopy (JEOL JEM 2100F, Tokyo, Japan).

The final setting times (ST) of the cement pastes were evaluated using the tip (1 mm diameter) of a Vicat needle with a 400 g load (according to ISO standard 1566), and fails to make a perceptible circular indentation on the surface of the cement.

The changes in concentration of released calcium and phosphate ions from cements during soaking cement pellets in SBF solution at 37 °C (400mg/15ml solution, polypropylene tube, shaken) were analysed by ICP (Horiba Activa) after filtration over membrane filter (PVDF, 45μm pore size, Millipore) at selected soaking times (0, 2, 4, 6, 24, 48 and 168 h).

2.3. Preparation of cement extracts and in vitro cytotoxicity testing of extract

For evaluation of contact cytotoxicity the cement samples (Ø 6 mm, 1 mm in thickness) were sterilized under UV light in laminar box for 30 min on each side of sample and placed in wells of 48–well culture plate (TPP, Trasadingen Switzerland). The mouse preosteoblastic MC3T3E1 Subclone 4 cells (ATCC CRL-2593, Manassas, VA, USA) were enzymatically released from culture flasks and the cell suspension was adjusted at a density $5.0x10^4$ cells/ml. To each tested sample were $2.0x10^4$ cells in 400 μl of culture medium (EMEM Mimimum essential medium + 10% FBS, 1% antibiotic solution) (all from Sigma) added. The density, distribution and morphology of the cells were assesed after 2 days of cultivation by live/dead fluorescent staining (fluorescein diacetate FDA/propidium iodide PI) by an inverted optical fluorescence microscope (Leica DM IL LED, blue filter).

To determine the cytotoxicity of the extracts, MC3T3E1 cells were resuspended in culture medium and the cell density was adjusted to 1.0×10^5 cells/ml in a vial. Briefly, 1.0×10^4 of mouse pre-osteoblasts were suspended in 100 μL of culture medium and seeded into each well of a 96-well cell grade Brand microplate (adherent wells) and cultured to a semi-confluent monolayer at 37 °C, 95% humidity, and 5% CO_2 in an incubator for 24 h. The cement pastes were immersed in culture medium (0.2 g/ml of culture medium) (according to ISO 10993-12:2012) [28] for 24 h at 37 °C. Subsequently, the culture medium in the wells was replaced with 100 μL of 100% extract. All experiments were carried out in triplicate, and cells in wells with extract-free complete culture medium were considered as the negative control (NC). After 24 h of culture, the extracts were replaced with fresh culture medium and the in vitro cytotoxicity was evaluated (ISO 10993-5:2009) [29] using the MTS proliferation test assay (Cell titer 96 aqueous one solution cell proliferation assay, Promega Madison, WI, USA) and a UV–VIS spectrophotometer (Shimadzu, Kyoto, Japan).

The determination of long-term cytotoxicity of cement-honey pastes has been carried out after 7 and 14 days of rat MSCs cultivation. The rat MSCs were isolated from femur and tibia s bone marrow. The MSC phenotype was confirmed by flow cytometry after staining of cell-specific markers (CD45/CD29/CD90.1, eBioscience, San Diego, CA, USA) as well as differentiated cells for the confirmation of their multi-differentiation capacities (StemPro Osteogenesis, Chondrogenesis and Adipogenesis Differentiation Kit (GIBCO), Waltham, MA, USA) [30].

For the long-term cytotoxicity testing of extracts (up to 14 days), the ratio of 0.1 g cement/mL medium was used. The cement pastes were soaked in complete osteogenic differentiation culture medium (α-modification Eagle's minimum medium, αMEM), 10% FBS, osteogenic supplements: 50 μg/mL of L-ascorbic acid, 50 nM dexamethasone, 10 mM β-glycerophosphate and 1% penicillin, streptomycin and amphotericin (all Sigma-Aldrich, Saint Louis, MO, USA) in an incubator at 37 °C for 24 h [28]. The rat MSCs passage 3 were resuspended in culture medium after harvesting by enzymatic digestion and cell density was adjusted to 5.0×10^4 cells/mL in a vial. Briefly, 2.0×10^4 of rat MSCs were suspended in 400 μL of EMEM + 10% FBS, 1% antibiotic solution and seeded into each well of a 48-well plate and cultured to a semi-confluent monolayer at 37 °C, 95% humidity, and 5% CO_2 in an incubator for 24 h. Subsequently, the culture medium in the wells was replaced with 400 μL of prepared extract (0.1 g/ml). All experiments were carried out in triplicate, and cells in the wells with extract-free complete culture medium were considered as the negative control (NC). Extracts were refreshed every two days.

The ALP activity of osteoblastic differentiated rat MSCs (after 7 and 14 days cultivation) was determined from cell lysates after lysis with solution containing 0.1% Triton X-100. The cell lysates were frozen at −20 °C, after thawing centrifuged at 10.000 RPM for 10 min. Aliquots of cell

Preprints (www.preprints.org) | NOT PEER-REVIEWED | Posted: 28 July 2023 doi:10.20944/preprints202307.1894.v1

supernatant were added to p-nitrophenyl phosphate in dietanolamine buffer, after incubation for 60 min at 37 °C was the amount of p-nitrophenol produced by the ALP enzyme catalysis determined from the calibration curve of p-nitrophenol at 405 nm using the UV VIS spectrophotometer. The ALP activities were expressed in micromoles of the p-nitrophenol produced per 1 min per microgram of proteins. The protein content in lysates was determined by Bradford's method with Coomasie blue G250 as the complexing agent.

The Alizarin red staining—staining of calcium deposits produced by differentiated osteoblasts, was done after 7 and 14 days of rat MSCs cultivation in extracts. Cells were washed with PBS, fixed in ethanol and washed with distilled water. Deposits were stained with Alizarin red S staining solution for 30 min. After removing the staining solution and washing three times with distilled water, the cells were observed under a light microscope (Leica DM IL LED, Heerbrugg, Switzerland).

2.3.1. Analysis of osteogenic Gene Expression in differentiated rat MSCs

The gene expression was analyzed according to method [7]. For the extraction of total RNA, 1.0×10^6 cells were used. Total RNA from each cell culture was extracted using a RNeasy Mini Kit (Qiagen, Germantown, MD, USA) following the manufacturer's instructions. Contaminating genomic DNA was digested using an RNase-free DNase set (Qiagen, Germantown, MD, USA). The RNA quality and yields were analyzed using a NanoDrop spectrophotometer (Thermo Scientific, WI, USA). Complementary DNA (cDNA) synthesis was performed using the protocol for the RT2First Strand Kit (Qiagen, Germantown, MD, USA), where 1 μg of total RNA was used (after the genomic DNA elimination step) to prepare 20 μL of cDNA, which was used for real time PCR experiments (RT PCR). The quantification of genes of interest in the cDNA samples was performed using primers for following genes: B-actin rat, type I collagen rat, osteocalcin rat, osteopontin rat and osteonectin rat (Table 1). A 25-μL reaction mixture, consisting of triplicate samples of cDNA, specific primer mix, and RT2 SYBR Green qPCR mastermix (Qiagen, Germantown, MD, USA) was setup in each well of a 96-well reaction plate (Roche, Basel, Switzerland). cDNA for β actin was used as the endogenous control for calculating fold differences in the RNA levels of cells treated vs. not treated with cement extracts according to the $2^{-\Delta\Delta CT}$ method. The plate was sealed using an optical adhesive cover (Roche, Switzerland) and placed in a LightCycler 480 II RT PCR system machine (Roche, Switzerland). RT PCR was performed under the following conditions: initial incubation at 95 °C for 10 min, amplification in 45 cycles at 95 °C for 15 s followed by 60 °C for 1 min. Amplification specificity was checked by generation of a melting curve.

Table 1. Forward (F) and reverse (R) primers of genes used for RT-PCR determination.

Genes	Primers	References
B-actin rat	F: GTAGCCATCCAGGCTGTGTT R: CCCTCATAGATGGGCAGAGT	[31]
Typ I collagen rat	F: CCAGCTGACCTTCCTGCGCC R: CGGTGTGACTCGTGCAGCCA	[32]
Osteocalcin rat	F: ACAGACAAGTCCCACACAGCAACT R: CCTGCTTGGACATGAAGGCTTTGT	[33]
Osteopontin rat	F: CCGATGAATCTGATGAGTCCTT R: TCCAGCTGACTTGACTCATG	[34]
Osteonectin rat	F: GGAAGCTGCAGAAGAGATGG R: TGCACACCTTTTCAAACTCG	[34]
Alkaline Phosphatase rat	F: AACCTGACTGACCCTTCCCTCT R: TCAATCCTGCCTCCTTCCACTA	[35]

Preprints (www.preprints.org) | NOT PEER-REVIEWED | Posted: 28 July 2023 doi:10.20944/preprints202307.1894.v1

2.3.2. Antibacterial Activity of cements and honey samples

The antibacterial activity of honey cement samples was investigated by using two bacterial strains: Gram-negative *Escherichia coli* ATCC 11303 and Gram-positive *Staphylococcus aureus* CCM 5776 (Czech Collection of Microorganisms, Brno, Czech Republic). *E. coli* ATCC 11303 *and S. aureus* CCM 5776 strains were inoculated onto the surface of nutrient agar (OXOID, UK) and cultured at 37°C for 24 h. From the 24-hour culture, the bacterial colonies were suspended in brain-heart infusion broth (BHI), and the turbidity was adjusted to 0.5 degree (1.0 x 10^8 CFU.ml^{-1}) according to the McFarland turbidity standard with a densitometer (BIOSAN, Latvia).

The tested samples were used in the following forms: 1 ml of undiluted medical honey, 1 g of TTCPM cement paste, 1 g of V10 or M10 paste. Pastes were prepared from sterile powders and liquids under aseptic conditions. 3 mL of BHI broth bacterial suspension was added to each freshly prepared sample and mixed. BHI broth (3 ml) with *S. aureus* and *E. coli* was considered as negative control (NC), BHI broth (3 ml) without bacterial strains was considered as blank. The final volume of bacterial suspension in all samples was 3 ml. The bacteria-samples were cultivated in an incubator at 37 ºC for 24 hours. After rigorously mixing was 200 µl suspension removed from each bacteria-cement suspension and transferred into 48 well plate and MTS reagent (Cell Titer Aqueous One Solution Cell Proliferation Assay, Promega, Madison, WI, USA) was added according to the manufacturers instruction. After 30 min incubation at 37 °C, the absorbance of formazan metabolised by active bacteria from tetrazolium was measured by UV VIS spectrophotometer at 490 nm (Shimadzu, Japan). The relative inhibition of bacterial activity was calculated as the difference between the NC formazan absorbance (set to 1 or 100%) and the ratio of the formazan absorbance reduced by the blank value in the tested samples to the NC formazan absorbance.

3. Results

3.1. XRD and FTIR analysis of cements

The XRD patterns of cements after hardening for 1 and 7 days in SBF at 37 °C are shown in Figure 1a,b. The nanocrystalline hydroxyapatite (HAP) (PDF4 01-071-5048) was identified in all patterns and none traces of other secondary phases arise from starting calcium phosphate components in origin powder cement mixture or their transformation after immersion to SBF were found. The chemical analysis of the final nanohydroxyapatite phase by ICP demonstrated formation of calcium deficient form hydroxyapatite with the Ca/P molar ratio equal 1.64±0.02. The average crystallite size of nanohydroxyapatite in hardened cement was calculated from line representing reflection of (002) HAP plane using the Scherrer´s equation. The results showed no dependence of crystallite size on addition of honey to cements and average crystallite sizes were around 29 and 33 nm for 1 and 7 days hardened cements, respectively.

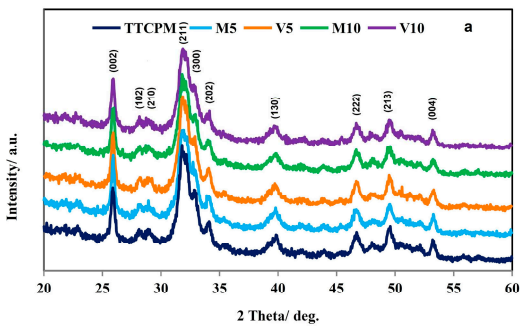

(**a**)

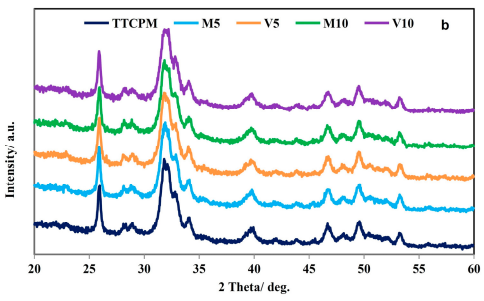

(**b**)

Preprints (www.preprints.org) | NOT PEER-REVIEWED | Posted: 28 July 2023 doi:10.20944/preprints202307.1894.v1

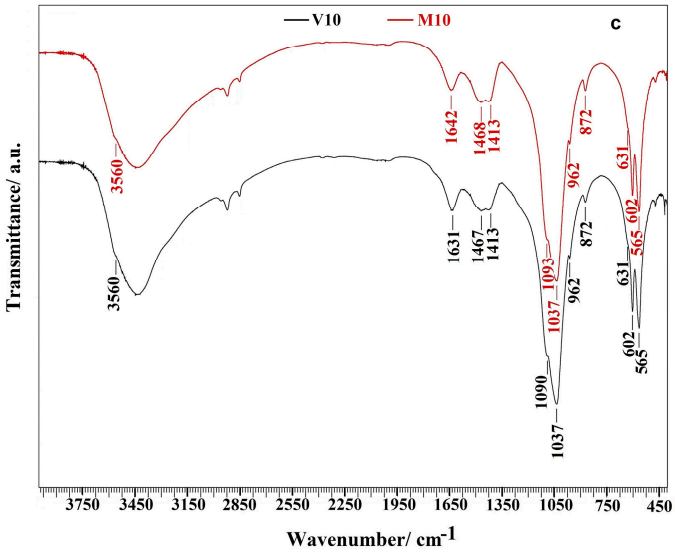

(c)

Figure 1. XRD patterns of TTCPM and honey cements after 1 (a) and 7 (b) days soaking at 37 °C in SBF (with assigned lines of HAP (PDF4 01-071-5048)) and FTIR spectra (c) of M10 and V10 cements after 7 days soaking at 37°C in SBF.

The FTIR analysis of M10 and V10 cements after 7 days soaking in SBF at 37 °C verified results from XRD analysis (Figure 1c). The insufficiently distinguished peaks characteristic for the stretching and librational modes of OH group at 3560 and 630 cm^{-1} in spectra clearly revealed nanocrystalline nature of HAP. Moreover, the presence of HAP confirmed peaks at 962 cm^{-1} (ν_1 stretching symmetric vibrations), 602 and 564 cm^{-1} (O–P–O bending vibrations from triplicate degenerate bending mode ν_4), 1090 and 1037 cm^{-1} (triple degenerated antisymmetric stretching mode ν_3) from PO_4^{3-} of hydroxyapatite [36]. In addition, bands at 1471, 1423, and 872 cm^{-1} representing asymmetric stretching ν_3 and ν_2 (out-of-plane bending) vibrational modes of carbonate group in B-type carbonated hydroxyapatite were found in all spectra [36,37].

3.2. Microstructure of cements and morphology of HAP particles in cements, setting time and compressive strength of cements

Microstructure of cements after hardening in SBF at 37 °C for 7 days is shown in Figure 2. A high fraction of fine 1-2 μm pores with several larger irregularly shaped macropores up to 10 μm in size were visible in the microstructure TTCPM cement (Figure 2a). HAP particles was joined to coarser and more compact globular agglomerates (up to 10 μm size) which were pulled out of the matrix after fracture. In addition, the HAP particles in the agglomerates had a rod-like morphology with a length of up to 400 nm, and a lower fraction of very fine particles of spherical morphology with submicron size was visible (Figure 2b). In the case of the honey cement samples, after pulling out the agglomerates from the cement matrix, a higher number of irregularly shaped micropores (size 2-3 μm) was identified in the microstructures (Figure 2 c, e), however, upon more detailed analysis (Figure 2 d, f), the images showed a columnar growth of long needle-like HAP particles (up to 1 μm in length). The columnary arranged particles formed walls around the original calcium phosphate (probably TTCP) particles, which were transformed into nanocrystalline HAP. Moreover, in detailed micrographs of M5 or V10 microstructures, agglomerates of newly formed HAP particles were often even separated from the surrounding matrix by a cement gap zone with a weak connection at the agglomerate/matrix boundary (Figure 2 j).

 doi:10.20944/preprints202307.1894.v1

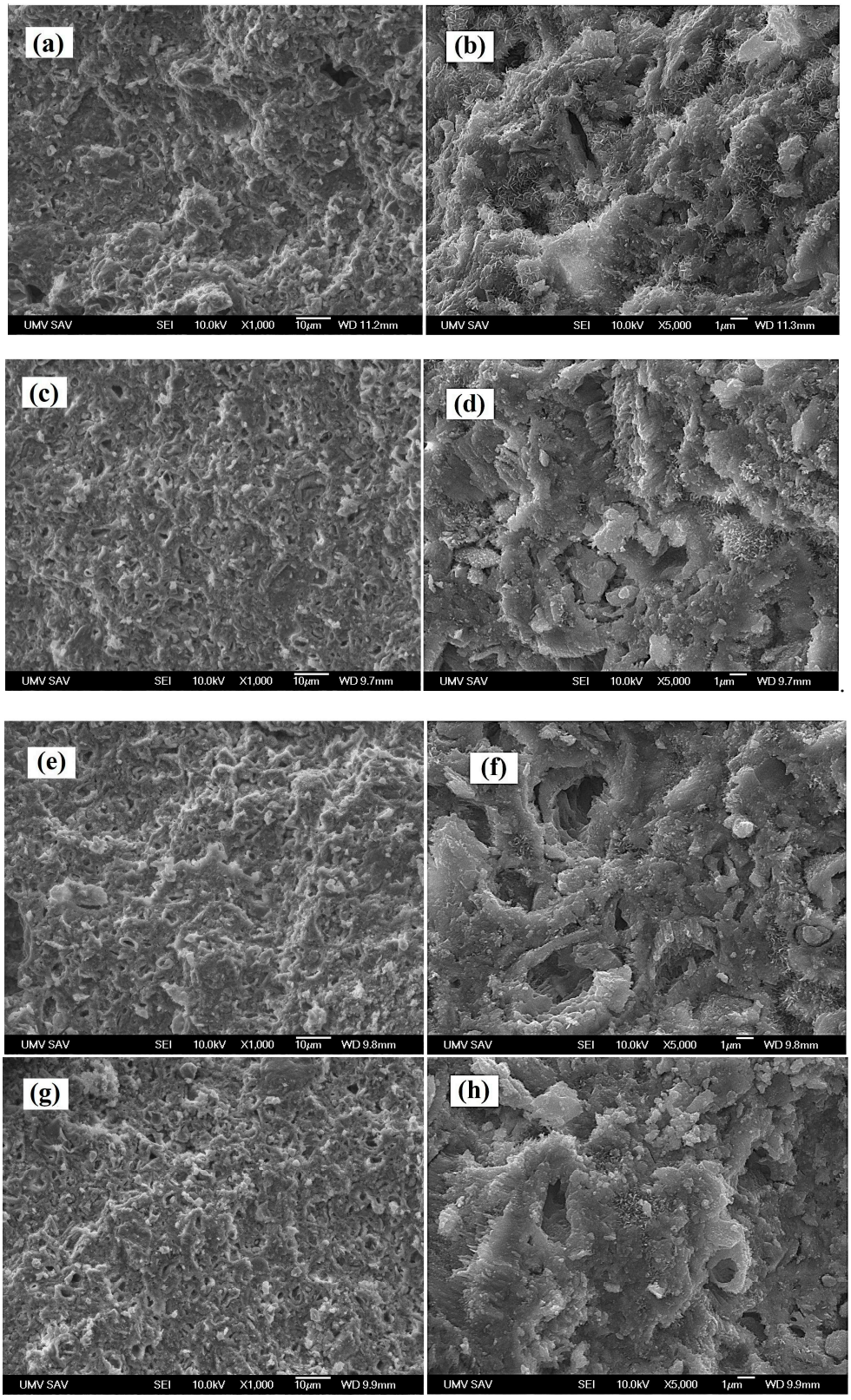

Preprints (www.preprints.org) | NOT PEER-REVIEWED | Posted: 28 July 2023 doi:10.20944/preprints202307.1894.v1

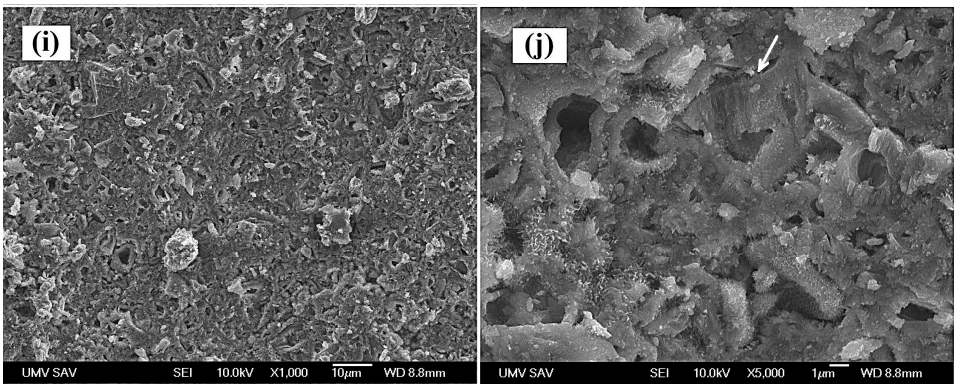

Figure 2. Microstructure of cements after hardening in SBF at 37 °C for 7 days (a,b – TTCPM; c,d – M5; e,f – V5; g,h – M10; i,j – V10). (arrow – columnar growth of HAP particles).

The morphology of HAP particles in M5 and M10 cements after 7 days soaking in SBF was characterized by TEM (Figure 3). The needle-like morphology of HAP prevailed in cements regardless the kind or concentration of honey in cement matrix. Besides lower number of very fine spherical HAP particles of 5-10 nm size was observed in cements. Remains of walls with columnary arranged needle-like HAP particles originally found in microstructures around pores can be found in Figure 3 c as the particle agglomerate of ~ 300 nm size.

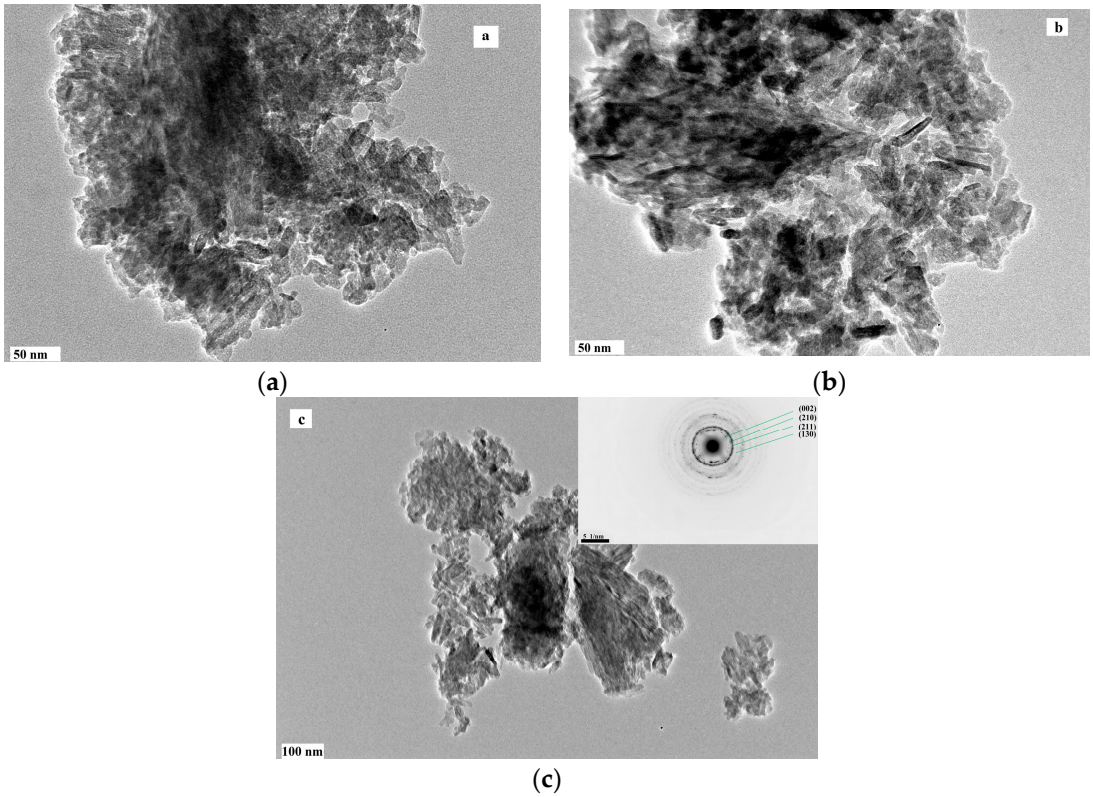

Figure 3. Morphology of HAP particles in cements after 7 days soaking at 37 °C in SBF (a – M5; b,c – M10; selected area electron diffraction in detail – HAP lines).

The aparent density of hardened cements was independent on addition of honey to cement and was close to 52±2% of theoretical HAP density. The CS of TTCPM cement was 42 ±2 MPa and decreased with 5 % (w/v) honey addition down to 35±5 MPa and 26±4 MPa for V10 and M10 cements, respectively. The final setting time of TTCPM and honey cements was 4±1 min and was independent on used honey additions.

Preprints (www.preprints.org) | NOT PEER-REVIEWED | Posted: 28 July 2023 doi:10.20944/preprints202307.1894.v1

3.3. Changes in pH and release of Ca and phosphate ions during soaking in aqueous solutions

The addition of honey to a liquid components insignificantly influenced their pH (close to 4.4). Measurement of pH changes during cement soaking in saline can help identify physicochemical processes that are not affected by the buffering capacity of any additives that are added to the SBF. It is clear from the comparison of individual curves in Figure 4 a,b that the dependences of pH on the soaking time of TTCPM and honey cements were different, despite the fact that it is possible to observe a rapid increase in pH up to 10.5 and 8.4 during the first 24 hours of soaking in NaCl and SBF, respectively, for TTCPM and honey cements with a subsequent stabilization for TTCPM (to 10.5 or 8.4 in NaCl and SBF) and a gradual decrease for honey cements (to 9.5 and 7 in NaCl and SBF).

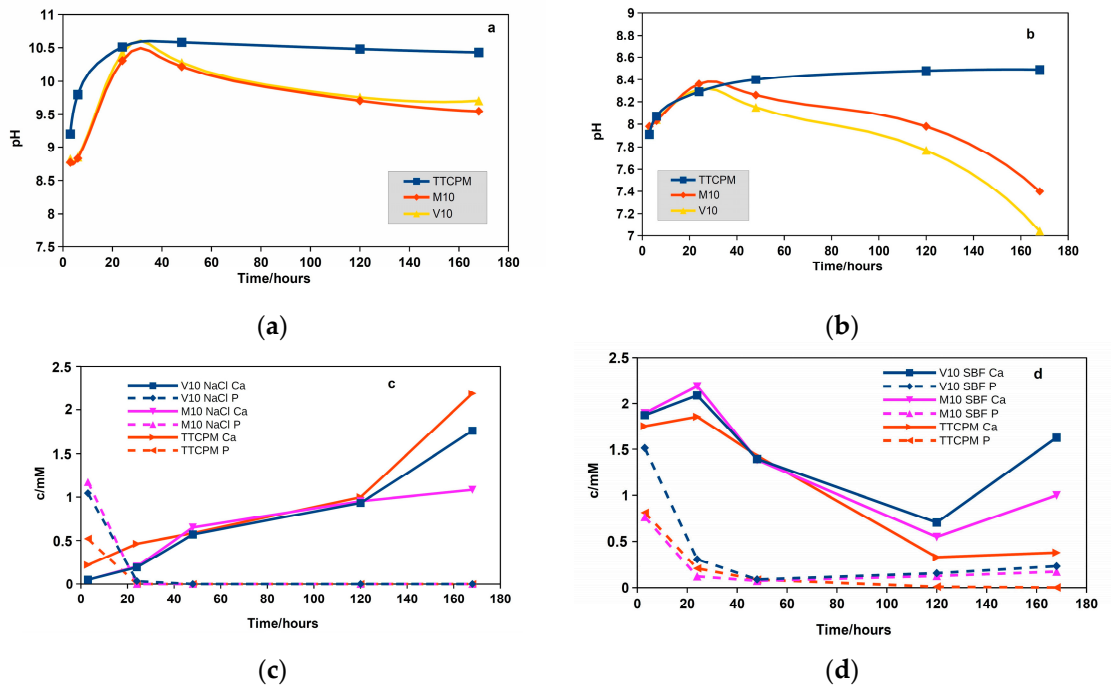

Figure 4. Changes in pH and calcium, phosphate ion concentrations of saline (a,c) and SBF (b,d) solutions during soaking of cements at 37 °C.

The changes in pH were accompanied with the fast reduction in phosphate concentration in both media (NaCl or SBF solutios) regardles the honey addition to cement (Figure 4 c,d). On the other hand, the calcium concentrations in NaCl solution rose with soaking time contrary to that in SBF solution where initially a small increase was found to about 2.2 mM after 24 hours, followed by a decrease to 0.8 and 0.5 mM after 120 hours from immersion for TTCPM and honey cements, respectively. During prolonged soaking time, the rise in calcium concentration was verified in solutions with honey cements whereas the Ca concentration in TTCPM SBF solution was almost constant (~ 0.3 mM).

3.4. Analysis of proteins, release of polyphenols and sugars from honey cements, antioxidant capacity of cement extracts

The total content of proteins in manuka and chestnut honey was 0.13±0.02 wt% and 0.07±0.015 wt%, respectively. The protein profiles of honeys determined by SDS PAGE electrophoresis are shown in Figure 5 a. The analysis revealed the presence of proteins with M_w equal 6, 10, 25, 55, 78, 110 and 160 kDa in both honeys but manuka honey contained a high portion of protein with M_w about 26 kDa. The identified proteins represent the major royal jelly proteins with M_w ~ 48-70 kDa, proteins originated from nectars or pollen between M_w 20-30 kDa and proteins with M_w 5 and 10 kDa can be assigned to apisimin and defensin-1 [38,39]. The total content of polyphenols in honeys determined colorimetrically was 1.45 and 0.99 mg/g of manuka and chestnut honeys, respectively. Moreover, the

Preprints (www.preprints.org) | NOT PEER-REVIEWED | Posted: 28 July 2023 doi:10.20944/preprints202307.1894.v1

content of flavonoids in manuka and chestnut honeys was 0.87 and 0.39 mg/g of honey. The amounts of selected polyphenols and flavonoids determined by HPLC method in both honeys are shown in Table 2.

Table 2. Contents of main polyphenols and flavonoids determined by HPLC method in honeys.

polyphenols	**chestnut [μg/g of honey]**	**manuka [μg/g of honey]**
Luteolin	8.2±1	3.9±1
Chrysin	55.6±6	26.1±3
Gallic acid	44.8±7	46.4±6
Kaempferol	18.1±2	6.9±1
3,4,5-trimethoxybenzoic acid	26.3±3	10.4±1
Chlorogenic acid	162.1±11	ND
Rutin	27.5±5	ND
Quercetin	7.5±1	4.3±1
Ferulic acid	26.8±3	12.9±2
Coumaric acid	76.0±6	32.4±2
Syringic acid	37.9±5	16.6±3
Methylsyringate	37.0±4	134.3±12
Caffeic acid	68.2±8	31.8±4
Protocatechuic acid	36.7±3	100.3±11
sugars	**[wt%]**	**[wt%]**
Fructose	50.1±2	40.5±2
Glucose	27.5±1	34.0±2
Saccharose	3.8±0.5	2.3±0.3
Maltose	5.7±0.8	4.8±0.8

The decrease in an amount of polyphenols and flavonoids released from honey cements was revealed during first 48 hours from immersion to physiological solution (Figure 5b). After 3 h soaking, about 70% and 42% of total amount of polyphenols was released to solution from M10 and V10 cements, respectively. On the other hand, only a very slow reduction in the amount of released polyphenols (2-5%) was identified from both cements and 15 and 32 % of polyphenols were released from V10 and M10 cements after 192 hours. In the case of cements extracts in SBF (Figure 5c), almost no difference in released polyphenols (around 30% of total phenols was released to SBF) between V10 and M10 was confirmed after 24 hours from immersion of cements. In addition, a gradual increase in the amount of released polyphenols with soaking time was observed for both cements, and ~60% of the total polyphenols were released into the SBF after 168 hours of soaking.

Preprints (www.preprints.org) | NOT PEER-REVIEWED | Posted: 28 July 2023 doi:10.20944/preprints202307.1894.v1

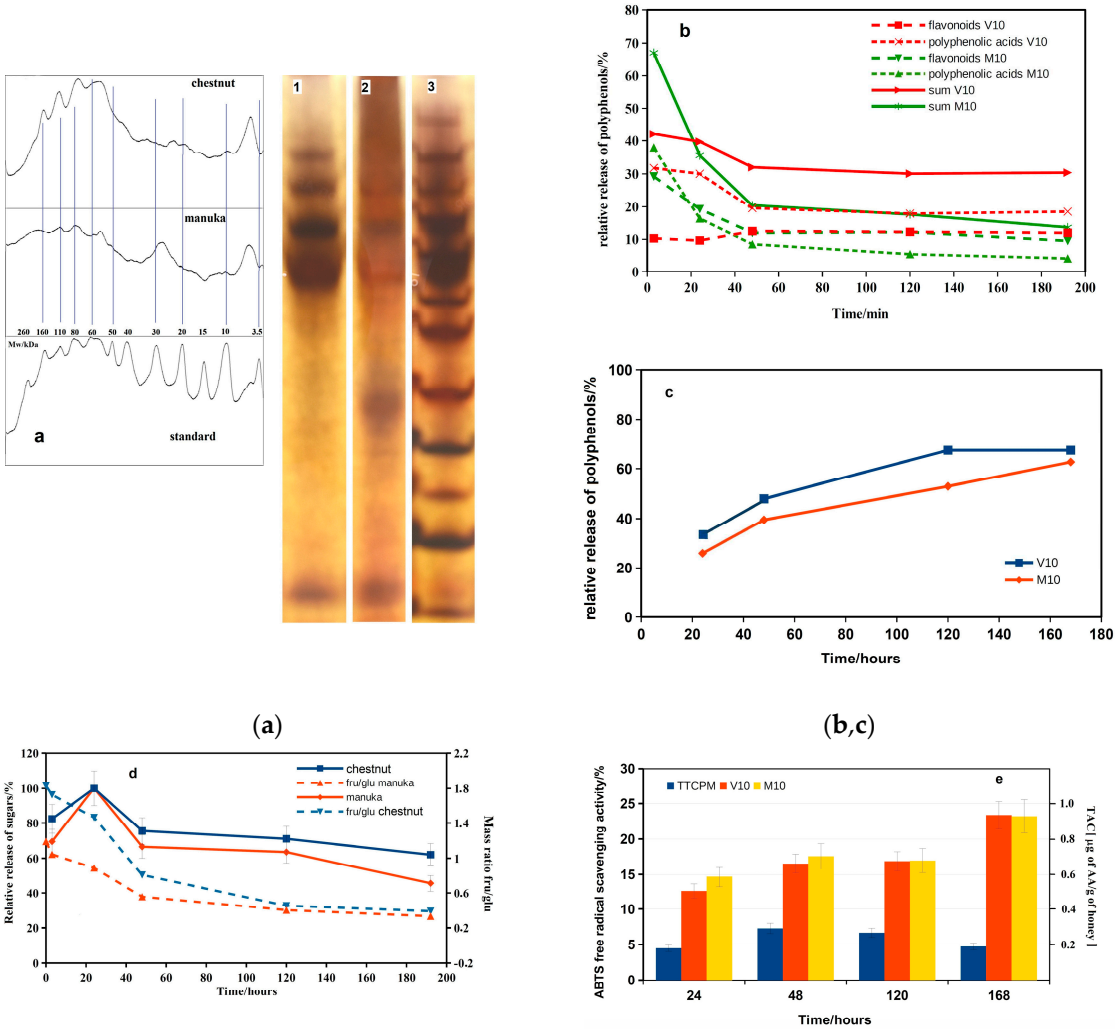

Figure 5. Protein profile of honeys determined by SDS PAGE electrophoresis (a) (lane 1:chestnut, lane 2: manuka, lane 3: standard); relative release of polyphenols and flavonoids from honey cements to physiological (b) and SBF (c) solutions; relative release of sugars and fru/glu mass ratio during soaking honey cements in physiological solution (d);. changes in ABTS free radical scavenging activities and TAC of SBF cement extracts with soaking time (e).

The contents of individual sugars in honeys are shown in Table 2. From the point of view of sugars (fructose (fru) and glucose (glu)), the 100% of total sugar content in cements was released into the physiological solution after 24 hours of immersion (Figure 5d). The released amount of sugars from M10 and V10 cements was rapidly reduced to about 65 and 75%, respectively, with following gradual decrease down to 45 and 63% during prolonged soaking for 192 hours. In addition, the fast fall in fru/glu mass ratio in extracts was measured during first 48 h of soaking from almost double higher content of fructose than glu (fru/glu=1.8) in chestnut honey to 0.8 in V10 extract with further gradual decline to ~ 0.4. Moreover, almost the same dependence of fru/glu mass ratio was found in manuka honey with a decrease in ratio to about 0.4 in M10 extract followed by further slow reduction to 0.3 after 192 h of soaking.

The free radical scavenging activities (FRSA) of chestnut and manuka honeys characterized 38±2 and 41±2 % of radical inhibition determined by DPPH method and 33±2 and 72 ± 3% by the ABTS method, respectively. In addition, TAC analysed using ABTS method were 1.30±0.05 and 2.76±0.05 mg of AA /g of chestnut and manuka honeys. The dependence of FRSA (ABTS method) of SBF cement extracts with soaking time (Figure 5e) revealed a gradual increase in value to about 17% after 48 hours

Preprints (www.preprints.org) | NOT PEER-REVIEWED | Posted: 28 July 2023 doi:10.20944/preprints202307.1894.v1

of soaking, and FRSA was confirmed to be almost stable up to 120 hours with a subsequent increase to about 23% after 168 hours of immersion. The TAC of SBF honey extracts achieved aprox. 0.9 mg of AA/g of honey after 168 h soaking.

3.5. In vitro cytotoxicity testing of cements and cement extracts, live dead staining, gene expression of cell in cement extracts

Before starting the experiments with honeys, the maximum concentration of honey in the liquid component of the cements was optimized based on the measurement of the medium cytotoxicity at different concentrations of honey in the medium (Figure 6a,b). Because the lowest noncytotoxic concentrations of honey were very different for chestnut and manuka honeys, the lower concentration equal to 3.125 g of honey/L of solution was selected as limity of possible cytotoxicity of cements for in vitro testing after immersion to solution. This fact corresponds to the applied max. 10% (w/v) honey content in the liquid component of the cement used to analyze the material properties of the cements, but in vitro testing was performed with cements containing 5% (w/v) honey in the liquid component so as not to use limit concentrations for cytotoxicity.

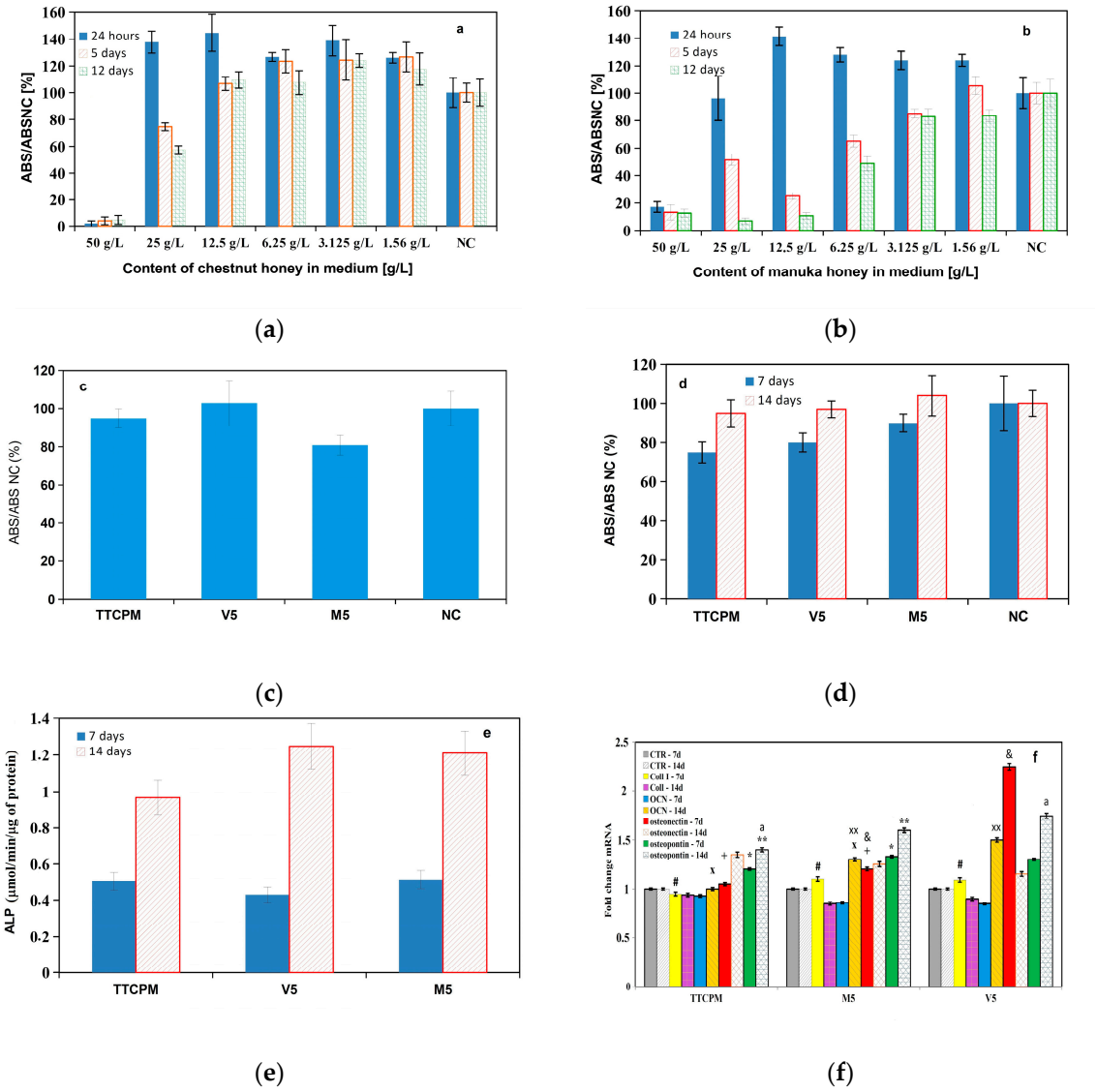

Figure 6. Cytotoxicity of medium at different concentrations of honey (a,b); cytotoxicity of TTCPM, V5 and M5 cement extracts after 24 h of soaking in MEM (c) and cultivation for 7, 14 days in osteogenic medium (d); ALP activities of MSC´s cultured in cement extracts for 7 and 14 days (e); RT PCR analysis of osteogenic gene expression in cells cultured in cement extracts for 24 h in MEM (f). (up regulation (osteocalcin (OCN), osteopontin (OP) in cells after 14 days (statistically significant difference, $p<0.001$)

Preprints (www.preprints.org) | NOT PEER-REVIEWED | Posted: 28 July 2023 doi:10.20944/preprints202307.1894.v1

and osteonectin (ON) genes (&: p<0.0001 for V5 extract) in cells cultured for 7 days in honey cement extracts) of osteogenic genes as compared with that in cells cultured in TTCPM extract).

No cytotoxicity of TTCPM, V5 and M5 cement extracts after 24 h of soaking in MEM was measured using MTS test according to ISO10993-5 [29] (Figure 6c) (where < 70% viability of cells in relation to NC was selected as cytotoxicity criterion for tested samples). From the point of view of long-term proliferation of rat MSC´s in extract, the strong rise in proliferation of cells with culture time in cement extracts was verified which revealed non cytotoxic character of extracts even in long time period of cultivation (Figure 6d). The ALP activities of MSC´s cultured in cement extracts rose with culture time and were aprox. double and almost triple for cells cultured in TTCPM, V5 and M5 extracts, respectively (Figure 6e). The increase in osteogenic potential of MSC´s during cultivation in both honey cement extracts indicated up regulation of osteogenic genes like osteocalcin (OCN), osteopontin (OP) after 14 days and osteonectin (ON) genes after 7 days cultivation in honey cement extracts (Figure 6f) as compared with cells cultured in TTCPM extract.

The images from live/dead staining (Figure 7 a,b,c) clearly demonstrate a good adherence of MC3T3E1 cells on surface of cement samples after 48 hours of cultivation where none dead cells were found. The density of cells and their distribution on the surfaces was almost identical for the cements, the cells were well spread and partially connected by filopodia, which confirmed the non-cytotoxic nature of the sample surfaces regardless of the type of cement. The alizarin red staining confirmed the ability of differentiated rat MSCs to produce calcium deposits (Figure 7 d-i).

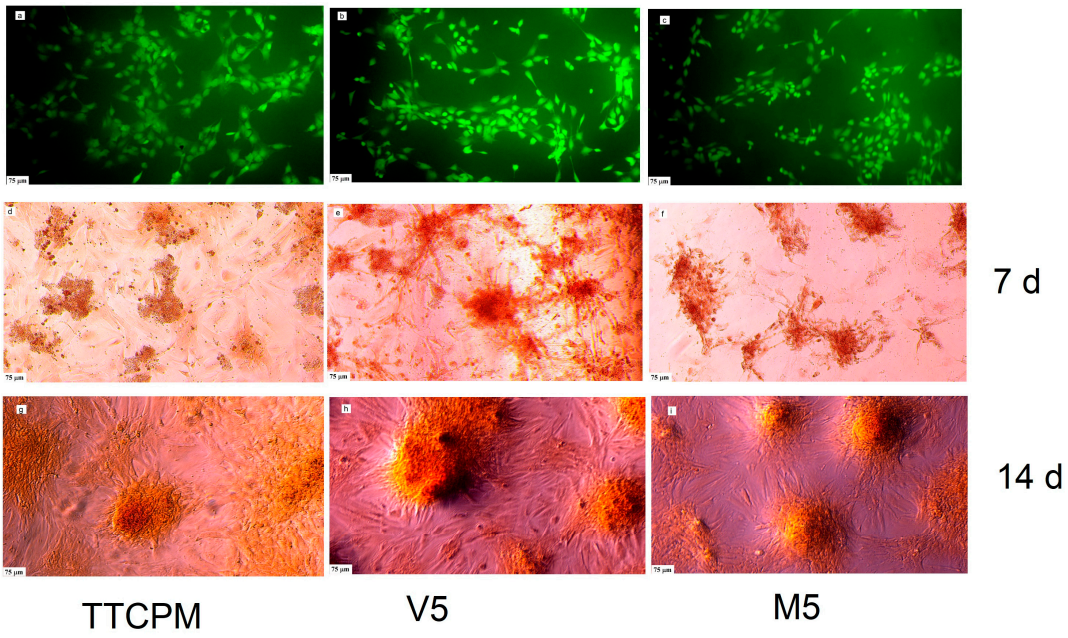

Figure 7. Live/dead staining of MC3T3E1 cells on surface of cement samples after 48 hours of cultivation in cement extracts (a-c); calcium deposits produced by cells cultured in cement extracts for 7 and 14 d stained by alizarin red (d-i).

3.6. Antibacterial activity of cements

The antibacterial activity of TTCP/honey paste was examined by using two bacterial strains: *Escherichia coli* as a Gram-negative and *Staphylococcus aureus* as a Gram-positive strain. The *E. coli* was more sensitive to cement extract and hardening liquid with honeys. The relative inhibition of bacterial activity (RIA) of all tested samples in case of *E. coli* represents an interval within a range of 55 -70 % in relation to NC contrary to *S. Aureus* where the RIA´s of V10 and M10 cement extracts were 12 and 5 % (statistically significant difference, p<0.05), respectively, while TTCPM extract had almost zero RIA. The liquid components with chestnut and manuka honeys had RIA´s of 55 and 70 % for *E. Coli* (statistically significant difference, p<0.05), and 65 and 30% for *S. Aureus*, respectively (Figure 8 a,b).

Preprints (www.preprints.org) | NOT PEER-REVIEWED | Posted: 28 July 2023 doi:10.20944/preprints202307.1894.v1

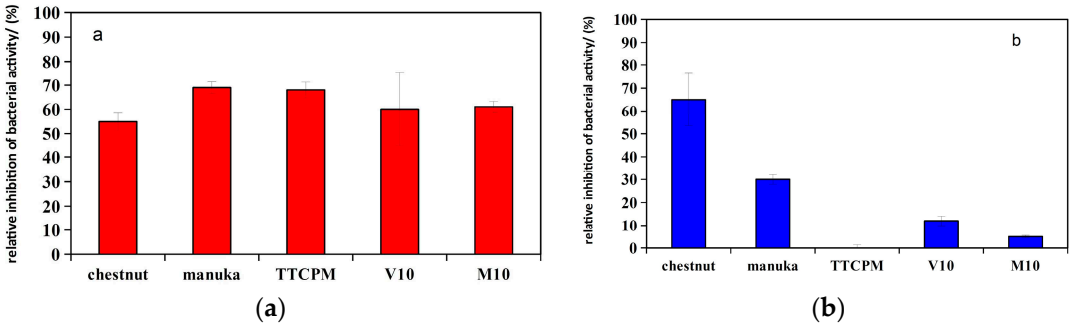

Figure 8. Relative inhibition of bacterial activity of *Escherichia coli* and *Staphylococcus aureus* in cement samples.

4. Discussion

To the best of our knowledge, there is practically no information in the literature about the influence of honey on the material characteristics or properties of CPC´s as well as on the behavior of osteoblastic cells in vitro after its addition to CPC´s. Honeys contain a high concentration of sugars, especially fructose and glucose, as measured in manuka and chestnut honeys with 82 and 87 wt% of sugars, respectively, while the fraction of other active ingredients, such as proteins, polyphenolic acids or flavonoids, did not exceed tenths of wt% . It is clear that the microstructure of honey cements can be affected by the above mentioned compounds. The monosaccharides effectively reduced the growth of HAP particles even in a very low concentration in supersaturated solutions of calcium phosphates during the precipitation due to both a strong affinity to HAP and the negative shift of zeta potential of particles [40]. The formation of needle-like HAP particles was demonstrated after adding of glucose to the reaction mixture under alkaline conditions at 70°C and results showed that the higher temperature of precipitation supported elongation and growth of HAP crystals along the c-axis [41]. On the other hand, stable complexes between Ca^{2+} or phosphate ions and glucose were verified in solutions during the HAP precipitation under neutral conditions which caused refining of HAP particles. Refinement and decrease of crystallity size in c-axis were even found after addition of glucose to freshly precipitated HAP particles where adsorbed glucose strongly interacts with OH groups in HAP and formation of calcium hydroxide and calcium carbonate was indicated [42]. Flavonoids reduced the crystallite size of HAP particles at low concentration in reaction solution during the neutralization reaction without preferential growth but no changes in morphology were confirmed after their adsorption on the surface of particles [43]. In the case of gallic acid as example of polyphenolic acid, the strong effect on crystallite size was revealed with formation of Ca/gallic acid complexes and an increase in the Ca/P ratio due to the replacement of phosphate functional groups in the crystal lattice was found [44]. Similarly, it was verified much effective inhibition of HAP precipitation as well as the HAP crystal growth in the presence of polyphenols with larger molecular weight (tannic acid, humic acid) as the result of energetically favorable adsorption on surface of HAP nuclei [45]. Note that the preferential oriented HAP along the c-axis was sythesized from αTCP by hydrothermal process using flavonoid – quercetin—as template in relative high amounts [46]. The crystallity size of HAP particles and setting process were not affected by the presence of honey during transformation process of TTCPM cement but morphology and recrystallization of HAP particles were influenced by the addition of honey. The columnary growth of long HAP particles with needle-like morphology was found in honey cements which could be related to the presence of monosaccharides in cement matrix. The rapid release of monosaccharides (up to 100% of total content in cement) was measured during first 24 h of setting honey cements in NaCl solution with a subsequent decrease to 70-80 % of total sugar content in cement after 48 h of soaking. Thus, approx. 20-30 % of sugars was adsorbed in hardened and transformed cement on surfaces of HAP particles when the origin calcium phosphate phases were transformed to nanohydroxyapatite. From above resulted that the low adsorption of glucose and fructose proceed on surfaces of active powdered calcium phosphate particles due to fast changes in chemical character and texture of surface of particles during hydrolysis of TTCP with formation of calcium hydroxide accompanied with the rise

in pH. Moreover, the nucleation of HAP particles followed the dissolution of monetite nanoparticles (change in phosphate concentration in solution) and mutual interaction. These processes clearly documented the dependences of the changes in concentration of calcium and phosphate ions during first 24 hours from immersion of cements to solutions where the rapid rise in phosphate concentration and slowly increase in calcium concentration was identified after 3 hours setting. It should be noted that the catalytic effect of HAP on transformation of monosaccharides can be probably predicted from measured fall of fru/glu mass ratio with soaking time. It is known that reducing sugars create α-dicarbonyl compounds followed calcium complexes [47] as well as glucose is isomerized to fructose which is more easily decomposed to lower organic acids and lowers the pH of media [48] which has been observed in honey cement extracts. Similar dependence was revealed in the case of polyphenols especially polyphenolic acids which were gradually disociated with increase of medium basicity and adsorbed on surface of HAP particles. These facts were supported by gradual decline in pH with prolonged soaking in both aqueous media due to the interaction of free hydrogen ions with hydroxide ions. On the other hand, the amount of released polyphenols to SBF increased with soaking time due to recrystallization of HAP which caused firstly, the loss of active surface on particles and secondly, the partial fall of ionization with increasing solubility of surface complexes and HAP nanoparticles in more acid SBF. It is clear that the formation of surface complexes decelerates the diffusion of ions on longer distances and local supersaturation related to HAP solubility constant is relative faster achieved at adjacent surfaces of particles surrounded more acidic environment, and recrystallization is also controlled with the participation of adsorbed chemical species to columnar form. The higher concentration of calcium ions found in SBF solutions after 168 h soaking of honey cements in comparison TTCPM cement verified above conclusion. In the case of soaking in NaCl solution, the Ca and phosphate concentrations were very close after fully transformation of starting calcium phosphates in cements and slowly rose with soaking time up to 120 hours but the solubility of HAP at almost steady state condition after 168 h soaking was desceding in order TTCPM>V10>M10 which corresponds with amount of polyphenols adsorbed on honey cements and resulted density of surface complexes. It should be noted that in addition to COOH groups, phenolic OH groups also dissociate at pH > 9 [45], which strengthen the surface interaction with calcium ions. On other side, a part of phenolic compounds is incorporated into HAP lattice and it is difficult to release them to solution [43].

The ABTS FRSA of honey extracts achieved about 23% of antioxidant inhibitory activity and TAC was close to 0.9 mg AA/g of honey which was about 30% and 70% of manuka and chestnut honey TAC, respectively. The changes in FRSA correlated quite well with an amount of released polyphenols (around 50% of total content) into SBF (linear regression coefficient equal 0.95 and 0.90 for V10 and M10 cements, respectively). However, the FRSA of the TTCPM extract increased significantly (more than threefold) after the addition of honey, indicating a direct effect of honey components on the antioxidant properties of cements. The both honeys had relative high TAC (1.3 and 2.7 mg AA/g of honey) as compared with Czech or Croatian monofloral honeys (0.4 mg AA/g of honey) but honeys from other sources (heterofloral, raspberry, honeydew etc.) had TAC up to 0.9 mg AA/g of honey. On the other hand, the total phenolic content was much lower in these honeys (especially in monofloral) excluding honeydew honey with 1.2 mg GA/g honey [49,50]. In the case of Algerian floral honeys with comparable phenolic contents (0.9-1.5 mg GA/g of honey) like in used manuka and chestnut honeys, similar ABTS antioxidant inhibitory activities equal ~20-50 % were found [25]. It is clear from above that despite the lower antioxidant inhibitory activity of honey in cement extracts than in pure honey solutions, ABTS FRSA was close to common monofloral or heterofloral honeys.

The main difference between Gram-negative and Gram-positive bacteria is in structure of the cell wall where a thick layer of peptidoglycane charcterizes Gram-positive and thin peptidoglycane surrounded by lipopolysacharide layer in outer membrane represents Gram-negative bacteria. These differences in structure cell wells can affect the sensitivity of bacteria to antibacterial substances including honeys. It has been shown that the addition of heavy metal ions like Ag, Zn, Bi to CPC [51–54] as well as the formation of specific nano/micro-topography on final cement surfaces (pillars, rod-

 doi:10.20944/preprints202307.1894.v1

or needle-like particles) can effectively enhance antimicrobial activity of CPC´s [55]. Moreover, the antibacterial activity was revealed for CPC´s in which calcium hydroxide is one of product of setting process for example in mixture of dihydrogen phosphate monohydrate and calcium oxide with sodium phosphate buffer as a liquid phase where the clear and reproducible bacterial growth inhibition was observed against all the microorganisms tested for cement samples with Ca/P ≥ 2 [56]. Similarly, inhibitory activity was observed for nanocrystalline tetracalcium phosphate cement with > triple inhibition zones for *S. Epidermidis* and *S. Salivarius* detected around the cement samples than for crystalline $Ca(OH)_2$ using agar diffusion tests due to the formation of amorphous $Ca(OH)_2$ in the cements [57]. Moreover, the inhibition efficiency of the micro-layered calcium hydroxide nanoparticles were 63% and 50% for *S. aureus* and *P. Putida*, respectively, and the reactive oxygen species mediated antibacterial proficiency was demonstrated [58]. The alkaline ions containing CPC´s showed a significantly higher antimicrobial efficiency (almost tenfold) than the commercial calcium hydroxide cement, which was a result of enhanced solubility of alkali metal phosphates and the subsequent formation of corresponding hydroxides with an increase in pH [59]. In the case of TTCMH cement, the pH of SBF solution and amount of calcium hydroxide increased during first 24 h from cement immersion but with addition of honey to cement, the gradual reduction was measured probably due to consumption of hydroxyl ions in solution. The RIA´s for *E.Coli* were close to 50-60% in all tested samples and from comparison resulted a small effect of honey addition on RIA. Therefore, the antibacterial activity of cements for *E.Coli* can be related to release of $Ca(OH)_2$ during cement transformation. Absolutely opposite results were revealed for *S. Aureus* where while antimicrobial activity for TTCPM cement was very low, V10 and M10 cements had RIA statistically significantly higher than 0 ($p<0.05$) but much lower than RIA of chestnut or manuka honey solutions (statistically significant difference, $p<0.001$). These facts showed a direct effect of the addition of honey on the antimicrobial properties of cements for *S. Aureus*, which may be a consequence of the amount of released phenols from the cements, the concentration of methylglyoxal or H_2O_2 in the extracts. Manuka honey has been shown to eradicate methicillin-resistant *S. aureus* as well as to have a synergistic effect with antibiotics to improve antimicrobial properties [60]. In addition, it had a higher antimicrobial activity against Gram-positive bacteria compared to Gram-negative bacteria (*E.Coli*) [61]. In the case of bioactive materials, the relative viability of bacteria in media with bioglass/methylcellulose foams after addition of 2.5 wt% of manuka honey significantly decreased, clear reduction of *S. Aureus*, and even a stronger effect was observed on *E. Coli* [62]. Moreover, the 45S5 bioactive glass-based scaffolds coated with corn protein zein and Manuka honey showed the antibacterial activity against *S. Aureus* with about 70% reduction in relative viability of strains after 8 h culture with foams containg 10 wt% of honey [63].

The in vitro cytotoxicity testing clearly demonstrated non-cytotoxic character of V5 and M5 honey cement extracts and supporting the proliferation of differentiated MSC´s in extracts. In addition, ALP activity and calcium deposit production by MSC´s were higher in honey extracts than in TTCPM extract. Enhanced differentiation of MSC´s into osteoblasts was verified by analysis of osteogenic gene expression of MSC´s cultured in honey cement extracts obtained after soaking in osteogenic medium with observed overexpression of OP and OCN genes after 15 days of culture and ON in V25 extract after 7 days of culture. It was found that the osteonectin is produced by active osteoblasts for supporting hydroxyapatite binding to collagens [64]. On the other hand, the OP enhances matrix mineralization and appropriate osteointegration of new bone tissue with mature bone and promotes osteoclasts anchoring to the mineral matrix of bones during biocement resorption [65,66]. Osteocalcin is the most abundant non-collagenous protein in bone and induces parallel growth of hydroxyapatite to the collagen fibrils, which is important parameter for bone strength [67]. From the point of view of osteogenic properties of honey, it was shown that flavones and flavonoids in honey have good osteogenic potential, promotes osteogenic differentiation of mesenchymal stem cells and accelerate bone fracture healing [68,69]. Therefore, the higher in vitro osteogenic activity of cells cultured in V25 or M25 extracts indicates a positive and synergistic effect of honey in conjunction with CPC, whereby the obtained composite system could be a promising therapeutic candidate for the repair of bone defects. Note that very little differences in properties were found between V and

M cements and statistically significant differences were only revealed in the expression of osteogenic genes (osteonectin, osteopontin and osteocalcin) with higher levels for V than M cement, which could be related to increased cytotoxicity manuka honey.

5. Conclusion

New biocements based on calcium phosphate/monetite powder mixture with the addition of honey were prepared and the influence of honey on the resulting properties of the cement was evaluated. It was shown that the setting process of cements was not affected by the addition of a liquid component containing honey in a non-cytotoxic concentration (up to 10% (w/v)) and the setting time of ~4 min corresponded to the fast setting CPC. The original calcium phosphate cement powder mixture was completely transformed into calcium-deficient nanohydroxyapatite after 24 hours of hardening in SBF. A higher fraction of long needle-like nanohydroxyapatite particles with columnar growth around the original TTCP phase particles was identified in the honey cements. The compressive strength of honey cements was reduced with the content of honey in the cement. The antibacterial activity of honey cements on *E. Coli* did not differ from the antibacterial activity of honey solutions or TTCPM cement, which may be related to the release of calcium hydroxide during cement transformation, but very low antibacterial activity was found for *S. Aureus* for all cements. It was shown that the antioxidant inhibitory activity of honey in cement extracts correlated with an amount of released polyphenols and was close to that of common monofloral or heterofloral honeys. In vitro MTS cytotoxicity testing identified the non-cytotoxic nature of V5 and M5 honey cement extracts as well as increased ALP activity and calcium deposit production by MSC´s in honey extracts. Analysis of osteogenic gene expression of MSC´s cultured in honey cement extracts confirmed the overexpression of OP, OCN and ON genes.

Author Contributions: L.Medvecky-Supervision, Investigation, Conceptualization, Formal analysis, Writing—Review & Editing, **M.Giretova** – Investigation, Writing—Original Draft, **R.Stulajterova**—Investigation, Writing—Original Draft, **L. Luptakova** – Investigation, Formal analysis, **T.Sopcak-** Investigation, **P.Jevinova-** Investigation.

Ethics approval and consent to participate: Animal or human experiments are not involved in this study.

Data availability Statement: Data will be made available on request.

Acknowledgments: The research was funded by the Slovak Research and Development Agency under the contract No. APVV-20-0184.

References

1. Kageyama, T.; Akieda, H.; Sonoyama, Y.; Sato, K.; Yoshikawa, H.; Isono, H.; Hirota, M.; Kitajima, H.; Chun, J.S.; Maruo, S.; Fukuda, J. Bone beads enveloped with vascular endothelial cells for bone regenerative medicine. *Acta Biomater*. **2023**, *165*, 168-179.
2. Wei, S.; Wang, Y.; Sun, Y.; Gong, L.; Dai, X.; Meng, H.; Xu, W.; Ma, J.; Hu, Q.; Ma, X.; Peng, J.; Gu, X. Biodegradable silk fibroin scaffold doped with mineralized collagen induces bone regeneration in rat cranial defects. *Int. J. Biol. Macromol*. **2023**, *235*, 123861.
3. Veronesi, F.; Martini, L.; Giavaresi, G.; Fini, M. Bone regenerative medicine: metatarsus defects in sheep to evaluate new therapeutic strategies for human long bone defect. A systematic review. *Injury* **2020**, *51*, 1457-1467.
4. Carey, L.E.; Xu, H.H.K.; Simon, C.G.; Takagi, S.; Chow, L.C. Premixed rapid-setting calcium phosphate composites for bone repair. *Biomaterials* **2005**, *26*, 5002-5014.
5. Takagi, S.; Chow, L.C.; Markovic, M.; Friedman, C.D.; Costantino, P.D. Morphological and phase characterizations of retrieved calcium phosphate cement implants. *J. Biomed. Mater. Res. (Appl. Biomater.)* **2001**, *58*, 36-41.
6. Medvecky, L.; Giretova, M.; Stulajterova, R.; Luptakova, L.; Sopcak, T. Tetracalcium phosphate/monetite/calcium sulfate hemihydrate biocement powder mixtures prepared by the one-step synthesis for preparation of nanocrystalline hydroxyapatite biocement – properties and in vitro evaluation. *Materials (Basel)* **2021**, *14*, 2137.

7. Medvecky, L.; Giretova, M.; Stulajterova, R.; Luptakova, L.; Sopcak, T.; Girman, V. Osteogenic potential and properties of injectable silk fibroin/tetracalcium phosphate/monetite composite powder biocement systems. *J. Biomed. Mater. Res.* **2022**, *110*, 668–678.
8. Nie, Y.; Wang, T.; Wu, M.; Wang, Ch.; Wang, J.; Han, Z. Enhanced bioactivity and antimicrobial properties of α-tricalcium phosphate cement via PDA@Ag coating. *Mat. Lett.* **2023**, *330*, 133230.
9. Yu, T.; Gao, Ch.; Ye, J.; Zhang, M. Synthesis and characterization of a novel silver-substituted calcium phosphate cement. *J. Mater. Sci. Technol*. **2014**, *30*, 686-691.
10. Kouassi, M.; Michaïlesco, P.; Lacoste-Armynot, A.; Boudeville, P. Antibacterial effect of a hydraulic calcium phosphate cement for dental applications. *J. Endodont*. **2003**, *29*, 100-103.
11. Valverde, S.; Ares, A.M.; Elmore, J.S.; Bernal, J. Recent trends in the analysis of honey constituents. *Food Chem*. **2022**, *387*, 132920.
12. Hossen, Md.S.; Ali, Md.Y.; Jahurul, M.H.A.; Abdel-Daim, M.M.; Gan, S.H.; Khalil, Md.I. Beneficial roles of honey polyphenols against some human degenerative diseases: a review. *Pharmacol. Rep.* **2010**, *69*, 1194-1205.
13. Abd-El Aal, A.M.; El-Hadidy, M.R.; El-Mashad, N.B.; El-Sebaie, A.H. Antimicrobial effect of bee honey in comparison to antibiotics on organisms isolated from infected burns. *Ann. Burns. Fire Disasters*. **2007**, *20*, 83-88.
14. Deng, J.; Liu, R.; Lu, Q.; Hao, P.; Xu, A.; Zhang, J.; Tan, J. Biochemical properties, antibacterial and cellular antioxidant activities of buckwheat honey in comparison to manuka honey. *Food Chem*. **2018**, *252*, 243-249.
15. Hossain, M.L.; Lim, L.Y.; Hammer, K.; Hettiarachchi, D.; Locher, C. A review of commonly used methodologies for assessing the antibacterial activity of honey and honey products. *Antibiotics* **2022**, *11*, 975.
16. Martinotti, S.; Ranzato, E. Honey, wound repair and regenerative medicine. *J. Funct. Biomater*. **2018**, *9*, 34.
17. Yupanqui Mieles, J.; Vyas, C.; Aslan, E.; Humphreys, G.; Diver, C.; Bartolo, P. Honey: An advanced antimicrobial and wound healing biomaterial for tissue engineering applications. *Pharmaceutics* **2022**, *14*, 1663.
18. Kamaruzzaman, M.A.; Chin, K.Y.; Ramli, E.S.M. A review of potential beneficial effects of honey on bone health. *Evid. Based Complement. Alternat. Med*. **2019**, *2019*, 8543618.
19. Effendy, N.M.; Mohamed, N.; Muhammad, N.; Mohamad, I. N.; Shuid, A.N. The effects of tualang honey on bone metabolism of postmenopausal women. *Evid. Based Complement. Alternat. Med*. **2012**, *2012*, 938574.
20. Martiniakova, M.; Kovacova, V.; Mondockov, V.; Zemanova, N.; Babikova, M.; Biro, R.; Ciernikova, S.; Omelka, R. Honey: A promising therapeutic supplement for the prevention and management of osteoporosis and breast cancer. *Antioxidants* **2023**, *12*, 567.
21. Zor, T.; Selinger, Z. Linearization of the bradford protein assay increases its sensitivity: theoretical and experimental studies. *Anal. Biochem*. **1996**, *236*, 302-308.
22. Csepregi, K.; Kocsis, M.; Hideg, E. On the spectrophotometric determination of total phenolic and flavonoid contents. *Acta Biol. Hung*. **2013**, *64*, 500-509.
23. Singleton, V.L.; Orthofer, R.; Lamuela-Raventos, R.M. Analysis of total phenols and other oxidation substrates and antioxidants by means of folin-ciocalteu reagent. *Methods in Enzymology* **1999**, *299*, 152-178.
24. Ferreira, I.C.F.R.; Aires, E.; Barreira, J.C.M.; Estevinho, L.M. Antioxidant activity of Portuguese honey samples: Different contributions of the entire honey and phenolic extract. *Food Chem*. **2009**, *114*, 1438–1443.
25. Otmani, A.; Amessis-Ouchemoukh, N.; Birinci, C.; Yahiaoui, S.; Kolayli, S.; Rodríguez-Flores, M.S.; Escuredo, O.; Seijo, M.C.; Ouchemoukh, S. Phenolic compounds and antioxidant and antibacterial activities of Algerian honeys. *Food Biosci*. **2021**, *42*, 101070.
26. Sadeer, N.B.; Montesano, D.; Albrizio, S.; Zengin, G.; Mahomoodally, M.F. The versatility of antioxidant assays in food science and safety—chemistry, applications, strengths, and limitations. *Antioxidants* **2020**, *9*, 709.
27. Re, R.; Pellegrini, N.; Proteggente, A.; Pannala, A.; Yang, M.; Rice-Evans, C. Antioxidant activity applying an improved ABTS radical cation decolorization assay. *Free Radical Biology & Medicine* **1999,** *26*, 1231–1237.
28. ISO 10993-12; Biological evaluation of medical devices—Part 12: Sample preparation and reference materials. International organization for standardization: Geneva, Switzerland **2012**.
29. ISO 10993-5:2009 ; Biological evaluation of medical devices—Part 5: Tests for in vitro cytotoxicity. International organization for standardization: Geneva, Switzerland **2009**.

30. Giretova, M.; Medvecky, L.; Petrovova, E.; Cizkova, D.; Danko, J.; Mudronova, D.; Slovinska, L.; Bures, R. Poly-hydroxybutyrate/chitosan 3D scaffolds promote in vitro and in vivo chondrogenesis. *Appl. Biochem. Biotechnol*. **2019**, *189*, 556–575.
31. Grässel, S.; Ahmed, N.; Göttl, C.; Grifka, J. Gene and protein expression profile of naive and osteo-chondrogenically differentiated rat bone marrow-derived mesenchymal progenitor cells. *Int. J. Mol. Med*. **2009**, *23*, 745–755.
32. Yang, J.; Chen, X.; Yuan, T.; Yang, X.; Fan, Y.; Zhang, X. Regulation of the secretion of immunoregulatory factors of mesenchymal stem cells (MSCs) by collagen-based scaffolds during chondrogenesis. *Mater. Sci. Eng. C* **2017**, *70*, 983–991.
33. Yusop, N.; Battersby, P.; Alraies, A.; Sloan, A.J.; Moseley, R.; Waddington, R.J. Isolation and characterisation of mesenchymal stem cells from rat bone marrow and the endosteal niche: A comparative study. *Stem Cells Int.* **2018**, *2018*, 6869128.
34. Karaoz, E.; Aksoy, A.; Ayhan, S.; Sarıboyaci, A.E.; Kaymaz, F.; Kasap, M. Characterization of mesenchymal stem cells from rat bone marrow: Ultra-structural properties, differentiation potential and immunophenotypicmarkers. *Histochem. Cell Biol*. **2009**, *132*, 533–546.
35. Sun, X.; Su, W.; Ma, X.; Zhang, H.; Sun, Z.; Li, X. Comparison of the osteogenic capability of rat bone mesenchymal stem cells on collagen, collagen/hydroxyapatite, hydroxyapatite and biphasic calcium phosphate. *Regen. Biomater*. **2018**, *5*, 93–103.
36. Ren, F.; Ding, Y.; Leng, Y. Infrared spectroscopic characterization of carbonated apatite: A combined experimental and computational study. *J. Biomed. Mater. Res. Part A* **2014**, *102A*, 496–505.
37. Grunenwald, A.; Keyser, C.; Sautereau, A.; Crubézy, E.; Ludes, B.; Drouet, C. Revisiting carbonate quantification in apatite (bio)minerals: A validated FTIR methodology. *J. Archaeol. Sci.* **2014**, *49*, 134–141.
38. Dżugan, M.; Miłek, M.; Sidor, E.; Buczkowicz, J.; Heclik, J.; Bocian, A. The application of SDS-PAGE protein and HPTLC amino acid profiling for verification of declared variety and geographical origin of honey. *Food Anal. Methods* **2023**.
39. Lewkowski, O.; Mures, C.I.; Dobritzsch, D.; Fuszard, M.; Erler, S. The effect of diet on the composition and stability of proteins secreted by honey bees in honey. *Insects* **2019**, *10*, 282.
40. Dalas, E.; Koutsoukos, P.G. The effect of glucose on the crystallization of hydroxyapatite in aqueous solutions. *J. Chem. Soc., Faraday Trans*. **1989**, *85*, 2465-2472.
41. Walsh, D.; Kingstone, J.L.; Heywood, B.R.; Mann, S. Influence of monosaccharides and related molecules on the morphology of hydroxyapatite. *J. Cryst. Growth* **1993**, *133*, 1-12.
42. Murillo, L.M.; Iessi, I.L.; Quintino, M.P.; Damasceno, D.C.; Rodrigues, C.G. Glucose is an active chemical agent on degradation of hydroxyapatite nanostructure. *Mat. Chem. Phys.* **2020**, *240*, 122166.
43. Palierse, E.; Masse, S.; Laurent, G.; Le Griel, P.; Mosser, G.; Coradin, T.; Jolivalt, C. Synthesis of hybrid polyphenol/hydroxyapatite nanomaterials with anti-radical properties. *Nanomaterials* **2022**, *12*, 3588.
44. Jerdioui, S.; Elansari, L.L.; Jaradat, N.; Jodeh, S.; Azzaoui, K.; Hammouti, B.; Lakrat, M.; Tahani, A.; Jama, C.; Bentiss, F. Effects of gallic acid on the nanocrystalline hydroxyapatite formation using the neutralization process. *J. Trace Elements and Minerals* **2022**, *2*, 100009.
45. Inskeep, W.P.; Silvertooth, J.C. Inhibition of hydroxyapatite precipitation in the presence of fulvic, humic, and tannic acids. *Soil Sci. Soc. Am. J.* **1988**, *52*, 941-946.
46. Liu, X.; Lin, K.; Qian, R.; Chen, L.; Zhuo, S.; Chang, J. Growth of highly oriented hydroxyapatite arrays tuned by quercetin. *Chem. Eur. J.* **2012**, *18*, 5519 – 5523.
47. Jaouia, W.; Hachimia, M.B.; Koutita, T.; Lacout, J.L.; Ferhata, M. Effects of calcium phosphate apatites on the reaction of reducing sugars in an alkaline medium. *Mat. Res. Bull*. **2000**, *35*, 1419–1427.
48. Patria, R.D.; Islam, Md K.; Luo, L.; Leu, S.Y.; Varjani, S.; Xu, Y.; Wong, J.W.C.; Zhao, J. Hydroxyapatite-based catalysts derived from food waste digestate for efficient glucose isomerization to fructose. *Green Synth. Catal*. **2021**, *2*, 356–361.
49. Lachman, J.; Orsak, M.; Hejtmankova, A.; Kovarova, E. Evaluation of antioxidant activity and total phenolics of selected Czech honeys. *LWT - Food Sci. Technol*. **2010**, *43*, 52-58.
50. Piljac-Žegarac, J.; Stipčević, T.; Belščak, A. Antioxidant properties and phenolic content of different floral origin honeys. *J. ApiProduct and ApiMedical Sci*. **2009**, *1*, 43 – 50.
51. Nie, Y.; Wang, T.; Wu, M.; Wang, C.; Wang, J.; Han, Z. Enhanced bioactivity and antimicrobial properties of α-tricalcium phosphate cement via PDA@Ag coating. *Mat. Lett.* **2023**, *330*, 133230.

52. Yu, T.; Gao, C.; Ye, J.; Zhang, M. Synthesis and characterization of a novel silver-substituted calcium phosphate cement. *J. Mater. Sci. Technol*. **2014**, *30*, 686e691.
53. Chen, F.; Liu, C.; Maoc, Y. Bismuth-doped injectable calcium phosphate cement with improved radiopacity and potent antimicrobial activity for root canal filling. *Acta Biomater*. **2010**, *6*, 3199–3207.
54. Fadeeva, I.V.; Goldberg, M.A.; Preobrazhensky, I.I.; Mamin, G.V.; Davidova, G.A.; Agafonova, N.V.; Fosca, M.; Russo, F.; Barinov, S.M.; Cavalu, S.; Rau, J.V. Improved cytocompatibility and antibacterial properties of zinc-substituted brushite bone cement based on β-tricalcium phosphate. *J. Mat. Sci: Mat. Med*. **2021**, *32*, 99.
55. Iglesias-Fernandez, M.; Buxadera-Palomero, J.; Sadowska, J.M.; Espanol, M.; Ginebra, M.P. Implementation of bactericidal topographies on biomimetic calcium phosphates and the potential effect of its reactivity. *Biomater. Adv*. **2022**, *136*, 212797.
56. Kouassi, M.; Michaïlesco, P.; Lacoste-Armynot, A.; Boudeville, P. Antibacterial effect of a hydraulic calcium phosphate cement for dental applications. *J. Endodon*. **2003**, *29*, 100-103.
57. Gbureck, U.; Knappe, O.; Hofmann, N.; Barralet, J.E. Antimicrobial properties of nanocrystalline tetracalcium phosphate cements. *J. Biomed. Mater. Res. Part B: Appl. Biomater.* **2007**, *83*, 132–137.
58. Samanta, A.; Podder, S.; Ghosh, C.K.; Bhattacharya, M.; Ghosh, J.; Mallik, A.K. Dey, A.; Mukhopadhyay, A. K. ROS mediated high anti-bacterial efficacy of strain tolerant layered phase pure nano-calcium hydroxide. *J. Mech. Behav. Biomed. Mat*. **2017**, *72*, 110–128.
59. Gbureck, U.; Knappe, O.; Grover, L.M.; Barralet, J.E. Antimicrobial potency of alkali ion substituted calcium phosphate cements. *Biomaterials* **2005**, *26*, 6880–6886.
60. Alvarez-Suarez, J.M.; Gasparrini, M.; Forbes-Hernández, T.Y.; Mazzoni, L.; Giampieri, F. The composition and biological activity of honey: A focus on manuka honey. *Foods* **2014**, *3*, 420-432.
61. Bazaid, A.S.; Alamri, A.; Almashjary, M.N.; Qanash, H.; Almishaal, A.A.; Amin, J.; Binsaleh, N.K.; Kraiem, J.; Aldarhami, A.; Alafnan, A. Antioxidant, anticancer, antibacterial, antibiofilm properties and gas chromatography and mass spectrometry analysis of manuka honey: A nature's bioactive honey. *Appl. Sci*. **2022**, *12*, 9928.
62. Schuhladen, K.; Mukoo, P.; Liverani, L.; Nescakova, Z.; Boccaccini, A.R. Manuka honey and bioactive glass impart methylcellulose foams with antibacterial effects for wound-healing applications. *Biomed. Mater*. **2020**, *15*, 065002.
63. Arango-Ospina, M.; Lasch, K.; Weidinger, J.; Boccaccini, A.R. Manuka honey and zein coatings impart bioactive glass bone tissue scaffolds antibacterial properties and superior mechanical properties. *Front. Mater*. **2021**, *7*, 610889.
64. Bondarenko, A.; Angrisani, N.; Meyer-Lindenberg, A.; Seitz, J.M.; Waizy, H.; Reifenrath, J. Magnesium-based bone implants: Immunohistochemical analysis of peri-implant osteogenesis by evaluation of osteopontin and osteocalcin expression. *J. Biomed. Mater. Res. Part A* **2014**, *102*, 1449–1457.
65. McKee, M.D.; Pedraza, C.E.; Kaartinen, M.T. Osteopontin and wound healing in bone. Cells Tiss. Organs. **2011**, 194, 313–319.
66. Termine, J.D.; Kleinman, H.K.; Whitson, S.W.; Conn, K.M.; McGarvey, M.L.; Martin, G.R. Osteonectin, a bone-specific protein linking mineral to collagen. *Cell* **1981**, *26*, 99–105.
67. Komori, T. Functions of osteocalcin in bone, pancreas, testis, and muscle. *Int. J. Mol. Sci.* **2020**, *21*, 7513.
68. Pan, F.F.; Shao, J.; Shi, C.J.; Li, Z.P.; Fu, W.M.; Zhang, J.F. Apigenin promotes osteogenic differentiation of mesenchymal stem cells and accelerates bone fracture healing via activating Wnt/b-catenin signaling. *Am. J. Physiol. Endocrinol. Metab*. **2021**, *320*, E760–E771.
69. Huo, J.F.; Zhang, M.L.; Wang, X.X.; Zou, D.H. Chrysin induces osteogenic differentiation of human dental pulp stem cells. *Experiment. Cell Res*. **2021**, *400*, 112466.